Biomed Microdevices (2016) 18: 11
DOI 10.1007/s10544-016-0035-5

Characterization of tight junction disruption and immune response modulation in a miniaturized Caco-2/U937 coculture-based *in vitro* model of the human intestinal barrier

Qasem Ramadan[1] · **Lin Jing**[1]

Published online: 26 January 2016

Abstract A microfluidic-based dynamic *in vitro* model of the human intestinal barrier has been constructed and characterized. The intestinal epithelial monolayer was mimicked by culturing caco-2 cells on a porous membrane in a double-layered microfluidic chip and interfaced with a co-culture of U937 as a model of immune responsive cells. The physiological flow was also mimicked by a continuous perfusion of culture media from the apical and basolateral side of the porous membrane. This dynamic "*in vivo*-like" environment maintains a continuous supply of cell nutrient and waste removal and create mechanical shear stress within the physiological ranges which promotes uniform cell growth and tight junction formation. The monolayer permeability to soluble ion changes after treating with LPS, and TNFα as indicated by the reduction of the TEER value. In addition, the immune competent caco-2/U937-based model allowed the investigating the role of the epithelial layer as a protection barrier to biological hazards as indicated by the suppressing of the pro-inflammatory cytokine expression.

Keywords *In vitro* · Tight junctions · Intestine · TEER

✉ Qasem Ramadan
alramadanq@ime.a-star.edu.sg

[1] Bioelectronics Laboratory, Institute of Microelectronics, Agency for Science, Technology and Research (A*STAR), Singapore, Singapore

1 Introduction

The gastrointestinal (GI) tract epithelium is a single-cell layer that forms the largest and most important barrier against the external environment. It regulates the absorption of nutrients, electrolytes, water and maintains an effective defense against intraluminal toxins, antigens, and enteric flora (Groschwitz and Hogan 2009). Furthermore, the vast majority of medications introduced into the systematic circulation are administered by the oral route and transported across the intestinal barrier which is considered one of the limiting factors for successful therapeutic delivery. The selective permeability of the epithelium is achieved through the formation of complex protein-protein networks that mechanically link adjacent cells and seal the intercellular space (Groschwitz and Hogan 2009; Resta-Lenert and Barrett 2009. The intercellular junctions comprise two major proteins, namely, the tight junctions (TJs) and the adherent junctions (AJs) (Graham et al. 2009). The TJs, which are composed of claudin family proteins, occludin, and other proteins, are the most apical junctions and determine the paracellular barrier properties (Furuse et al. 1993; Ikenouchi et al. 2005; Furuse et al. 1998). On the other hand, AJs are basal to the TJs and primarily formed by E-cadheren, catenins, and actin filaments. These protein junctions provide the strength necessary to hold the cells together and form a continuous epithelium (Pappenheimer 1993). The permeability of the intestinal epithelial barrier is regulated in response to physiological and pathophysiological stimuli (Graham et al. 2009) which makes it the subject of an intensive investigation to study regulatory mechanisms and drug pharmacokinetics. It is believed that paracellular

transport plays a critical role in health and disease, where the increase of paracellular permeability allows water and nutrient absorption. On the other hand, increased paracellular permeability is well recognized in patients with inflammatory bowel diseases (Hollander et al. 1986; May et al. 1993).

Intestinal absorption is frequently modeled *in vitro* using a monolayer intestinal cell lines mainly, caco-2 and HT-29/B6 (Wikman-Larhed and Artursson 1995; Hilgendorf et al. 2000; Nollevaux et al. 2006). In particular, caco-2 cell culture has been established as a reliable model representing intestinal barrier properties and extensively used to predict apparent permeability coefficient of drugs (Yazdanian et al. 1998; Ungell and Karlsson 2003). Caco-2 cells is a colon cancer cell line which differentiate to form morphology similar to human small intestine; including brush border microvilli on the upper side of the monolayer that extend perpendicularly to the surface of the monolayer (Brand et al. 2000). The monolayer develops asymmetrically, and contains both TJs and brush border associated enzymes (Gan and Thakker 1997). When cultured on microporous membranes, caco-2 cells expose their apical side to the upper compartment and the basolateral side to the lower one (Halleux and Schneider 1991; Brand et al. 2000).

Recent developments in microfabrication and microfluidics technologies provided the tools to create advanced cell culture/co-culture systems "organs-on-a-chip", aiming to provide *in vivo*-like cellular microenvironments (Huh et al. 2011; Kim et al. 2012; Ramadan et al. 2013). A clear advantage of using microfluidic systems is the control of the fluid flow in physiologically-relevant dimensions, which makes it possible to regulate nutrient and drug concentrations at the levels of single cells. Perfusion-based media supply allows delivery and removal of soluble molecules into the cell microenvironment and controlled shear stresses by the fluid flow. These tools are therefore well suitable for studying the biological interactions down to the cell and molecular levels and have tremendous potential to be applied to study human physiology and pathogenesis, by effectively creating microphysiological models of human organs.

In this paper, we describe a dynamic microfluidic-based *in vitro* model of the human intestinal barrier that is integrated with a co-culture of immune cell model to form an immune-competent model of the human intestine. The system has been demonstrated by employing two cell lines namely caco-2 as a model of the intestine barrier and U937 as a model of the immune responsive cells. Constructing a physiologically relevant biological model within an integrated microfluidic system would allow a quantitative analysis of the interaction between the intestinal barrier, pharmaceutical stimuli and the immune system demonstrating the potential of the "organs-on-a-chip" technology in narrowing the clear gap between *in vivo* and *in vitro* studies. In particular, we highlight here the potential of using the Transepithelial Electrical Resistance (TEER) method as a useful endpoint for quality control assessment to describe barrier function in combination with perfusion based-microfluidic culture system as well as *in situ* inflammatory cytokine detection as a powerful tool for screening of paracellular transport in epithelia.

2 Materials and methods

2.1 Device design, fabrication and cell culture setup

The microfluidic device, which comprises an array of five cell culture chambers, was fabricated by assembling four polymer layers: two patterned poly(methyl methacrylate) (PMMA) sheets, a polystyrene (PS) sheet and a polydimethylsiloxane (PDMS) sheet (Fig. 1a). Figure 1b shows a detailed schematic view of a single chamber structure (the PDMS and PS layers are not shown). The microfluidic chambers and channels were cut into a 1 mm thick PMMA sheet which was previously laminated by a double-sided tape (3M, USA). Polyethylene terephthalate (PET) membrane (Millipore, Singapore) with a pore size of 0.4 μm was sandwiched between the two patterned PMMA sheets. This assembly creates a double–layered fluidic chamber with two vertically stacked compartments which are termed as the apical and basolateral compartments, separated by a porous membrane. To seal the fluidic device, the lower PMMA sheet was bonded to a PS sheet (0.5 mm) and to allow gas exchange through the chip the upper chamber was bonded to a PDMS sheet with a thickness of 1mm. An additional downstream compartment (immune assay compartment) is connected to the basolateral compartment for sampling the supernatant for subsequent immune assay and detection. The fluidic inlets of the culture chambers were connected to culture media reservoir through a set of PEEK tubing while the fluidic outlets were connected to a set of syringe (5 mL). The fluidic setup was structured to allow storing the culture media reservoirs inside the cell culture incubator to maintain steady culture environment (i.e. temperature and O2 supply) during experiments. Negative pressures were applied to the compartments using a set of syringe pumps (Harvard Apparatus, USA) positioned outside the culture incubator to maintain continuous perfusion of cell culture media through the cell culture chambers. The perfusion was maintained through the course of cell culture at a flow rate of 10-20 nL/s. The media flow independently in the apical and

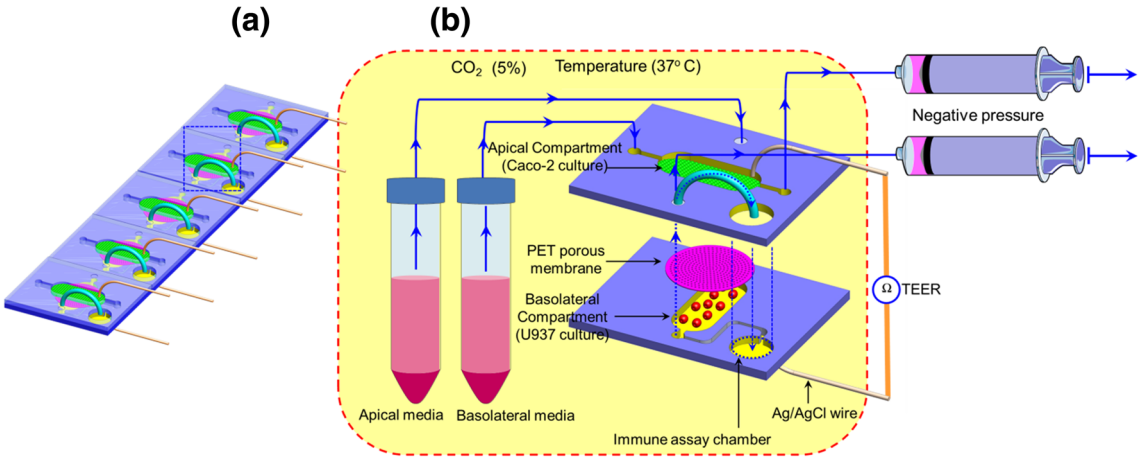

Fig. 1 (**a**) Schematic drawing of the cell culture chamber array (**b**) Detailed view of a single chamber of the perfusion setup. The fluidic chamber comprises two fluidic compartments separated by a porous membrane. The basolateral compartment is connected to a sampling reservoir for continuous collecting and sampling of the basolateral supernatant. The TEER is measured by inserting an AG/AgCl in both the apical and basolateral compartments and connected to a Volt-Ohm meter. The fluid was driven by a set of syringe pumps which apply a negative pressure to a set of media reservoirs positioned inside the cell culture incubator

basolateral compartments and no pressure difference was applied across the membrane. Ag/AgCl wires with a diameter of 0.5 mm (World Precision Instruments INC., USA) were inserted into the upper and lower compartments (above and beneath the PET membrane, respectively) by punching holes in the PDMS and PMMA sheets to measure the TEER of the epithelial cell (EC) layer in order to monitor the cell layer confluence and to assess the intercellular TJ integrity through the course of cell culture experiments.

2.2 Cell culture

The human intestine epithelium is modeled by a confluent layer of caco-2 cells (CLS Cell Lines Service GmbH, Germany) that is cultured on top of a porous membrane. The cells from 10-15 passages were maintained in a culture medium composed of Dulbecco's modified Eagle's medium (DMEM) with 4.5 mg/mL glucose, 50 U/mL penicillin, 50 U/mL streptomycin, 4 mmol/L glutamine, 25 mmol/L HEPES, and 10 % fetal bovine. Prior cell inoculation, the chips were wiped with 70 % ethanol, dried in the oven for 30 min at a temperature of 70 °C followed by UV irradiation for another 30 min. The chips were then filled with culture medium and pre-incubated overnight. After filling the culture chambers with fresh media, caco-2 cells were seeded at $\sim 10^5$ cells per cm^2 into the upper chamber using a syringe pump, and the media flows were completely stopped to allow cell attachment onto the membrane. After 2-5 hours, steady flows of culture media were driven by the syringe pumps at a flow rate of 10-20 nL/s. The microfluidic culture was maintained at 37°C in a humidified incubator with 5 % CO2.

2.3 Cell viability

A mixture of calcein-AM (2 μM) and ethidium homodimer-1(4 μM) which was diluted in D-PBS was injected into the upper chamber and incubated in the cell culture incubator for 10 min. Then the cell culture was examined by fluorescence microscopy. Cell viability was quantified by the percentage of calcein AM-labeled cells. Images were taken at least ten different observation locations and the percentage value was averaged. Data were represented as mean $\pm$SD.

2.4 TEER measurements

Ag/AgCl wires were sterilized by flushing with 70 % ethanol and UV irradiation prior inserting into the chip through the PDMS lid. The wires were then connected to Millicell® ERS-2 Volt-Ohm meter (Millipore, USA). TEER measurements were obtained at regular intervals with each data point being a mean of three measurements taken per culture chamber. The contribution of the membrane and culture medium is accounted for by subtracting the electrical resistance of the porous membranes without cells from the sample values and normalized with respect to the culture surface area by multiply the net electrical resistance by the total surface area covered by the caco-2 cells to calculate TEER in $\Omega.cm^2$.

2.5 Immunofluorescence staining of intercellular tight junctions

TJ staining was conducted one-week post-confluence when TEER value of more than 1000 $\Omega.cm^2$was reached. Cells were rinsed with PBS and fixed in 3.7 % formaldehyde at room temperature for 20 min. The cell layer was then rinsed in PBS and permeabilized in 0.2 % Triton X-100 for 10 min at room temperature. Cells were then rinsed in PBS followed by blocking with 1 % bovine serum albumin (BSA) for 30 min at room temperature. Cells were incubated with 2μg/mL anti-mouse occludin (Life Technologies, Singapore) at 4 °C overnight. After that, cells were washed with PBS and incubated with anti-mouse IgG conjugated to FITC (Life Technologies, Singapore) at room temperature for one hour. After washing with PBS, the membrane, with the cell layer, was detached from the chip and mounted on a microscope glass slide and stored at 4 °C in the dark until analyzed. The fluorescence TJ stain was visualized using Olympus fluorescent microscope (Olympus, BX3-CBH, Japan).

2.6 Paracellular permeability measurement

The apical-to-basolateral transport flux that is correlated to the paracellular transport route has been quantified by measuring the transport of fluorescein isothiocyanate (FITC)-4kDa dextran (Life Technologies, Singapore) through the caco-2 cell monolayer as a flux tracer. 10 μg/mL solution of FITC-dextran was added at the apical side of the monolayer, and the paracellular flux of the tracer molecule was quantified by serially sampling fluid from the basolateral compartment at different time intervals, and the tracer concentration was determined using Enspire fluorescent plate reader (Perkin Elmer, USA).

2.7 Caco-2/U937 co-culture

To examine the influence of the paracellular permeability to endotoxin and subsequent activation of immune cells, the caco-2 monolayer was interfaced with a co-culture of U937 cells in the basolateral compartment. U937 cells (Addexbio Biotechnologies, San Diego, USA), with a concentration of 2×10^5 cell/mL were seeded in the basolateral compartment after one week of caco-2 cells seeding and assuring the formation of a fully confluent monolayer. The U937 cells were also maintained in the same media of the caco-2 cells and kept in a static fluidic environment for 24 hours. Meanwhile, the perfusion flow was maintained in the caco-2 culture compartment. After 24 hour U937 cells were treated with phorbol myristate acetate (PMA) (Sigma-Aldrich, Singapore) with a concentration of 100ng/mL for 24 hours to initiate the differentiation to macrophages. Cells formed small clusters and attached to the surface of the chip after 24 hours of stimulation which confirms the differentiation to macrophages. The co-culture was then connected to the media perfusion circuit. Three-tiered culture system was experimented on the same chip that includes: caco-2 monoculture, U937 monoculture, and caco-2/U937 co-culture.

2.8 Cell stimulation and cytokine detection

Cells were treated with either LPS, or a combination of LPS and TNFα and the basolateral TNFα were quantified using magnetic bead-based immune assay employing the Milliplex Map, Human Cytokine magnetic bead panel, Cat # HCYOMAG-60k (Millipore, Singapore). Prior conducting the cytokine immune assay on the chip, serial dilutions of TNFα standards with known concentrations were prepared, and cytokine detection in a 96-well plate was conducted according to the manufacturer instruction. However, the fluorescent signals were measured using fluorescent plate reader instead of using the Luminex system. Therefore, bead color was not detected. Cytokine secretion was measured from the 3-tiered cellular setup on the same chip. The number of U937 cells which were used in the experiment is within the range of 500-1000 cells per chamber. The basolateral compartment of each chamber was connected to the corresponding downstream immune assay compartment (Fig. 1) where cell culture supernatant is collected for $\sim$ 24 hrs. Streptavidin-coated magnetic beads were incubated off-chip with biotinylated cytokine capture antibodies in PBS for 30 min. The antibody-coated magnetic beads were then separated from the supernatant by placing the tube on a magnet plate for 5 min and magnetically washed three times in PBS. The separated antibody-bead complexes were re-suspended to a concentration of 2×10^5 beads/mL and injected in the corresponding immune assay compartment. The stimulus was injected into the upper compartment and incubated in the cell culture incubator overnight. The supernatant from the basolateral compartments, where the immune cells are cultured, was allowed to infuse into the immune assay compartment during the incubation time. A small NdFeB magnet with diameter and height of 3mm and 2mm respectively was positioned under the immune assay compartment to retain the beads. After washing, streptavidin-PE conjugated cytokine detection antibodies were injected into the immune assay compartment containing the magnetic beads and incubated with the sample for 2 hours. Then, the magnetic bead/cytokine/streptavidin-PE complexes were washed with PBS and the fluorescent signal was measured using a fluorescent microscope. Images were analyzed using ImageJ software.

3 Results and discussions

3.1 Device fabrication, simulation and characterization

The micro-device was designed to mimic the structure of the transwell^{TM} culture plate which consists of two vertically stacked compartments separated by a porous membrane. The double layer structure allows perfusion of cell culture media and feeding the epithelial cells with nutrients from both the apical and basolateral sides. In this configuration, the culture media is continuously replenished in the compartments and infused through the membrane where the apical and basolateral compartments intersect. To emulate the physiological fluid flow, the fluidic compartments were integrated with a net of fluidic channels to maintain dynamic perfusion-based cell culture for extended periods of time. The porous membrane, which was previously treated for tissue culture, was obtained from the commercial sterile Transwell^{TM}. Each chip comprises an array of 5 identical and independent cell culture chambers which enabled 5 parallel assays.

All experiments in the current study including, the cell culture, the barrier characterization, the permeability and cytokine detection assays on-chip were conducted in a dynamic perfusion environment. The flow profiles, as well as the resultant shear stresses, were simulated using finite element analysis (COMSOL Multiphysics, Stockholm, Sweden) by solving Navier–Stokes equations to obtain the fluid velocity and shear stress profiles within the cell culture compartments and based on these calculations

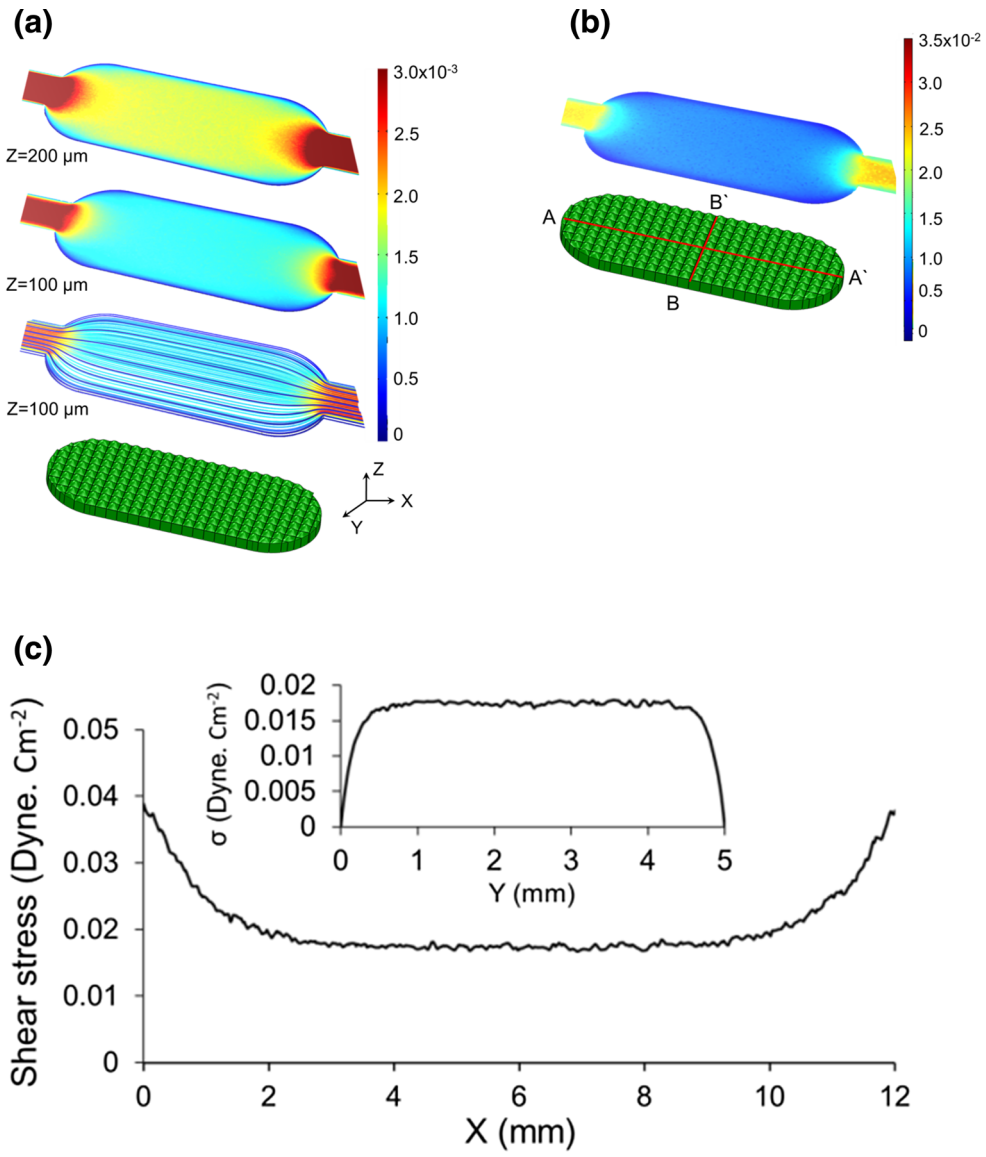

Fig. 2 Finite element analysis of the fluid flow inside the fluidic compartments. (**a**) The fluid velocity profile in the cell culture compartment at a plane located at 100 and 200 μm above the compartment bottom surface. The velocity profile at an inlet flow of 1 μL/min is uniform. (**b**) Uniform distribution of shear stress on the apical surface of the epithelial cells. (**c**) Uniform shear stress is maintained at $\sim$ 0,02 Dyne.cm^{-2} when the flow rate of 1 μL/min was applied at the compartment inlet. The shear stress calculated along the AA$^{`}$line in x-direction and BB$^{`}$in y-direction (*in the inset*). The flow rate was considered as 1 μL/min

the perfusion fluid flow were applied to the cell culture. Solving Navier–Stokes equations is a preferable option to describe the velocity, pressure and density of a moving fluid which are fulfilled in the microfluidic channels that we used in our study. A fully developed velocity profile was applied at the compartment inlet with a maximum flow rate of 2 μL/min. Three-dimensional, incompressible, Newtonian fluid flow with no slip conditions were applied at the inlets as well as ate the compartment walls. The fluid within the micro-device was assumed water without the presence of cells. Figure 2a shows the fluid velocity profile at two different planes (100 and 200 μm) above the compartment bottom surface. The simulation results show that the velocity profile is uniform across the fluidic compartment except at the inlet and outlets. Also, the resultant shear stress was found to be distributed evenly across the compartment as shown in Figs. 2b and c. The uniform distribution of velocity profile and shear stresses promotes uniform cell growth profile.

3.2 The *in vitro* model of the intestinal barrier

Caco-2 cells were seeded in the apical compartments of the cell culture array at a concentration of $\sim$ (1-5)$\times$ 10^5 cell/mL and incubated in the cell culture incubator. The fluidic compartments were connected to media reservoirs

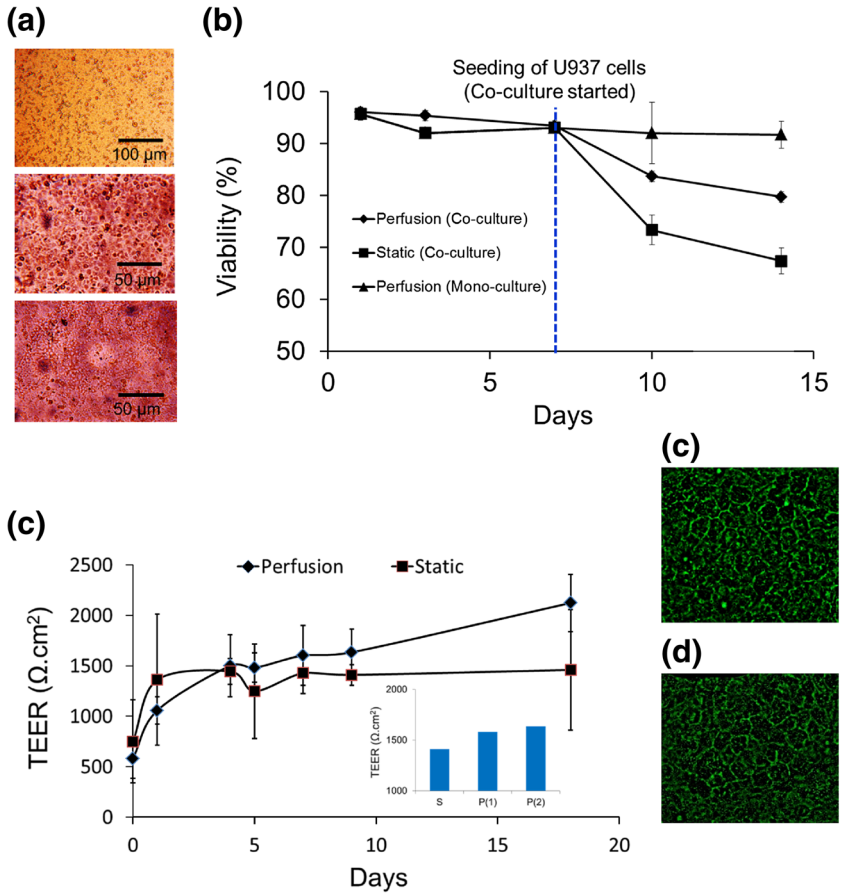

Fig. 3 (**a**) Optical images of caco-2 culture after 1, 4 and 18 days of seeding. A fully confluent monolayer was formed after 4 days of cell culture. (**b**) Caco-2 cell viability drops from $\sim$ 94 % immediately before u937 seeding to $\sim$ 75 % on day 10 after 3 days of co-culture with U937 in the case of static culture. But, in the perfusion cell culture, cells maintain higher viability in co-culture where the viability drops from 95 % to 83 % after 3 days of co-culturing with U937. The viability of caco-2 monoculture was maintained high ($>$ 90 %). (**c**) The perfusion-based culture showed higher TEER value after the formation of the confluent layer which suggest that perfusion accelerates the TJ formation and maintain healthier TJs over an extended period of culture comparing to static culture. TEER value was further increased when the media were perfused through both the apical and basolateral fluid inlets compared to perfusion through the apical side (*inset*). P1 refers tp perfusion through the apical side while P2n refers to perfusion through both apical and basolateral sides. (**d** and **e**) No obvious difference was observed in the tight junction staining between the dynamic and static culture. Perfusion was maintained at a flow rate of 10-20 nL/s

using manifolds. The fluid perfusion through the apical and basolateral compartments were driven by two independent syringe pumps so that the flow conditions can be selectively modulated for a different condition or switched ON/OFF. The cell growth in the microdevice was monitored visually to ensure the formation a fully confluent monolayer and TEER was measured every 12 hours. A fully confluent monolayer of caco-2 cells was observed after 4-5 days after cell seeding (Fig. 3a). Cells appeared to cover the entire membrane surface from the fourth day and beyond and maintained cell viability of >90 % for 14 days (Fig. 3b). Upon introducing the U937 cells into the basolateral compartment (after 7 days from the cell seeding), the caco-2 cell viability dropped from ~ 94 % to ~ 75 % in after 3 days of cell static co-culture. In the case of perfusion co-culture, cells maintained higher viability, where the viability drops from 95 % to 83 % after 3 days of co-culturing with U937 (Fig. 3b). This demonstrates the importance of the dynamic cell culture condition over static culture in modeling the interaction between various cell/tissue types.

The formation of a fully confluent monolayer that covers the entire membrane is essential for evaluating the caco-2 layer as a barrier model of the intestinal barrier and therefore to conduct permeability assays. To investigate the effect of perfusion flow on the caco-2 monolayer integrity and TJ formation, the perfusion flow was applied to selected cell culture chambers while other chambers were kept in static conditions where the culture media were manually changed every 24 hours. The TEER was measured in both cell culture systems in parallel. As in Fig. 3c, the measured TEER in the perfusion-based culture showed a higher value than that in the static system, particularly after the formation of the confluent layer (i.e. after 4 days of cell seeding). TEER reached > 1500 $\Omega.cm^2$ after 3 days of culture (Fig. 3c) and continued to increase up to 18 days in perfusion conditions while it stabilizes after one week of culture in the case of static culture. This may be attributed to the continuous replenishing of cell nutrients and removal of cellular waste. These data are consistent with previously reported using the same cell model (Kim et al. 2012; Ramadan et al. 2013). In addition, it was observed that cell growth and confluence were accelerated when the media were perfused through both the apical and basolateral fluid inlets compared to perfusion only through the apical side (Fig. 3c (inset)). The tight cellular monolayer was visualized by staining the TJ occludin (Fig. 3d and e). No obvious difference was observed in the TJ staining between the dynamic and static culture. All subsequent experiments were conducted after assuring void-less monolayer (after one week). Cells in the perfusion system may respond to the fluid shear stress through mechanotransduction mechanism that affects cell-cell adhesion and TJ expression. Ting et al. (2012) reported that endothelial cells under laminar flow had traction forces that were higher than those under static conditions. Furthermore, it was recently reported that shear-stress sensing involves many various types of membrane-associated molecules including the adhesion molecules (Ando and Yamamoto 2013). Our results on the epithelial cells are in agreement with these reported findings.

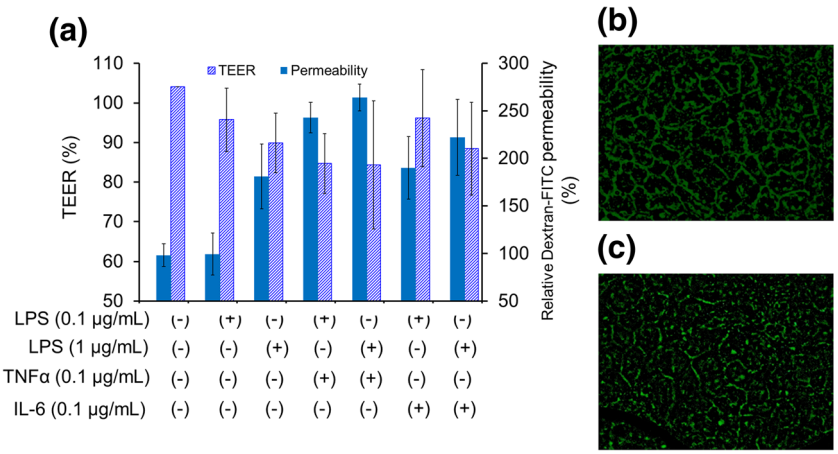

Fig. 4 Modulation of tight junction by LPS and cytokines. (**a**) The combination of LPS and TNFα or IL-6 significantly influence the TEER value, where the cell treatment with a combination of LPS/NFα and LPS/IL-6 reduces the TEER value to ~ 85 % of its original value. (**b** and **c**) Tight junction staining appears as dotted lines after treating the caco-2 monolayer with LPS. (**d**) The treatment of the cell monolayer with a combination of LPS and TNFα or IL-6 increases the paracellular FITC-dextran flux ~ 2.5 folds of its original value. The experiments were conducted in dynamic cell culture condition at a flow rate of 10-20 nL/s

3.3 Tight junction and permeability modulation in caco-2 monoculture

The caco-2 monolayer in the perfused monoculture was treated/co-treated with LPS and TNFα, and the TEER was measured after 24 hours of the treatment. One chamber in each chip was kept without treatment as a control. TEER dropped to ~ 80 % of its original value after stimulating the monolayer with LPS at a concentration of 1μg/mL (Fig. 4a). While co-treatment with a combination of LPS and TNFα or IL-6 significantly influence the TEER value, where the cell co-treatment with LPS/TNFα and LPS/IL-6 reduces the TEER value to ~ 85 % of its original value. These data are consistent with previously reported using the same cell model (Guo et al. 2013). Large variation of measurements was observed due to the variation of the Ag/AgCl wires positioning (distance from the cell layer) and alignment.

The LPS- and cytokine-induced modulation of TEER triggered an increase in the apical-to-basolateral transport (permeability) (Fig. 4a). It is generally accepted that the disturbance of the epithelial TJs promotes higher paracellular permeability to soluble ions. The apical-to-basolateral transport of FITC-Dextran was found to be significantly influenced by TEER variation. LPS or LPS/ TNFα/IL-6-induced reduction of TEER was accompanied by an increase of the relative permeability to FITC-Dextran (Fig. 4a). While stimulation of the cell monolayer with 0.1 μg/mL shows no influence, the permeability of the monolayer increases up to 1.84 folds at concentration of 1 μg/mL. On the other hand, co-stimulation the monolayer with LPS (1 μg/mL)/ TNFα (0.1 μg/mL) and LPS (1 μg/mL)/ IL-6(0.1 μg/mL) increases the permeability up to 2.7 and 2.3 folds, respectively. This was also confirmed by the occludin staining (Figs 4b and c). While the TJ staining appeared as continuous filaments before treatment (Fig. 4 b), it appears as dotted filaments after treating with LPS (Fig. 4c). These results also are in agreement with published data by Leonard et al. (2010).

3.4 Immune response of U937 to stimulation through caco-2 monolayer

A defective intestinal barrier is an important pathogenic factor of inflammatory bowel disease and other inflammatory conditions of the gut. Despite its importance in mediating intestinal inflammation, the physiological effects of LPS on the intestinal epithelial barrier remain unclear. Firstly, To evaluate the role of the caco-2 cell monolayer as a protection barrier against exogenous invasion, a 3-tiered culture namely, caco-2 monoculture, U937 monoculture and caco-2/U937 co-culture, was treated with LPS and the expression of the pro-inflammatory cytokines TNFα was quantified in the basolateral compartment of each culture chamber using the magnetic bead-based immune assay. LPS, with a concentration of 1μg/mL, was applied equally to the upper compartment of the three systems and incubated for 24 hours and the immune assay was performed to quantify the amount of secreted TNFα in the basolateral compartment. A significant increase of TNFα secretion was observed in the basolateral media of U937 monoculture comparing to that of caco-2 monoculture (Fig. 5a). A moderate increase of cytokine expression was observed upon treating the caco-2/U937 co-culture with LPS. These results suggest that the caco-2 monolayer forms a robust barrier against LPS invasion. The inflammation state in the barrier model was further induced by apically applying LPS and TNFα onto the caco-2/U937 co-culture, and the induced TNFα secretion was measured in the basolateral supernatant in the

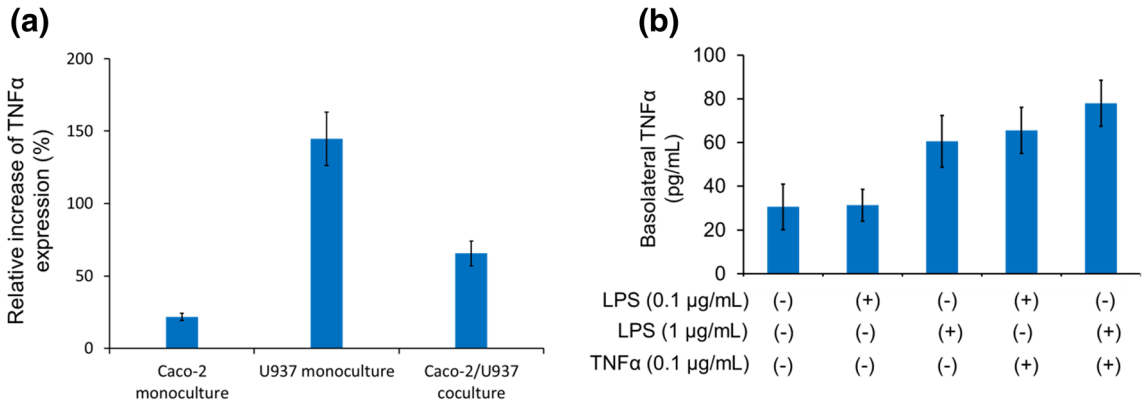

Fig. 5 (**a**) Significant increase of TNFα secretion was detected in the basolateral media of U937 monoculture in the absence of epithelial caco-2 barrier, comparing to that of caco-2 monoculture. This suggests that the caco-2 monolayer forms a robust barrier against LPS invasion. Effect of LPS and cytokine on stimulation of U937 through the caco-2 monolayer. (**b**) TNFα activity increases significantly upon treating the co-culture with LPS and combination of LPS and TNFα. The experiments were conducted in dynamic cell culture condition at a flow rate of 10-20 nL/s

immune assay compartment after 24 hours. A significant increase of TNFα was observed after co-stimulation of the co-culture with the LPS/TNFα (Fig. 5b). TNFα expression increased up to 2.6 folds when the co-culture was co-treated with LPS (1μg/mL) and TNFα (0.1μ g/mL) while it increased to 1.9 folds when the co-culture was treated only with LPS (1μg/mL). It is not clear whether; the disturbance of the tight junction and increasing the apical-to-basolateral permeability enhances the transport of TNFα molecules through the monolayer. Further investigations are required to understand the dual role of TNFα as a stimulator and inflammatory biomarker.

The objective of this work was to demonstrate the construction of miniaturized and dynamic *in vitro* model of the human intestinal barrier for high throughput experimentation and to investigate the effect of the endotoxin LPS and cytokines on TJ modulation. The modulation of the TJs of the intestinal barrier was studied by monitoring the variation of TEER upon treatment of various LPS and TNFα, occludin staining, permeability assay and immune cell activation in co-culture. The feasibility of the construction of an immune competent model of the intestinal barrier was also demonstrated. The barrier permeability can be selectively altered by the LPS and cytokines. These results demonstrate the potential of microfluidic-based *in vitro* modeling of human tissue "organs-on-a-chip" on our understanding of diseases, nutrient and drug absorption, as well drug discovery.

4 Conclusions

A dynamic miniaturized *in vitro* model of the human intestinal barrier has been demonstrated and characterized. The continuous perfusion of culture media into the cell culture in a double-layered structure enhanced the tight junction formation as evidenced by measuring higher values of TEER comparing to static culture. The fully confluent monolayer of the caco-2 cell responses to LPS and TNFα stimulation by increasing the permeability to soluble ion as indicated by the decrease in the TEER value which could be contributed to the down-regulation of the tight junction proteins. In addition, the immune competent caco-2/U937-based model also allowed the investigating the role of the epithelial layer as a protection barrier to biological hazards. This micro system has the potential to be developed as a useful tool for drug screening and toxicity.

Acknowledgments This research was supported by the Agency for Science, Technology and Research (A*STAR) (Grant number: 1431AFG123).

References

L. Ungell, J. Karlsson, In Drug bioavailability; Estimation of Solubility, Permeability, Absorption and Bioavailability, ed. by H. van de Waterbeemd, H. Lennernas, P. Artursson. (Wiley-VCH 2003), (2003), pp. 90–131

A. Wikman-Larhed, P. Artursson, Eur. J. Pharm. Sci. **3**, 171–183 (1995)

C. Halleux, Y.J. Schneider, in *Vitro. Cell Dev. Biol*, Vol. 27, (1991), pp. 293–302

C. Hilgendorf, H. Spahn-Langguth, C.G. Regårdh, E. Lipka, G.L. Amidon, P. Langguth, J. Pharm. Sci. **89**, 63–75 (2000)

D. Hollander, C.M. Vadheim, E. Brettholz, G.M. Petersen, T. Delahunty, J.I. Rotter, Ann. Intern. Med. **105**, 883–885 (1986)

D. Huh, G.A. Hamilton, D.E. Ingber, Trends Cell. Biol **21**(12), 745–54 (2011)

F. Leonard, E.M. Collnot, C.M. Lehr, Mol. Pharm. **7**(6), 2103–2119 (2010)

G. Nollevaux, C. Devillé, B. El Moualij, W. Zorzi, P. Deloyer, Y.J. Schneider, O. Peulen1, G. Dandrifosse, BMC Cell Biol. **7**(20) (2006)

G.R. May, L.R. Sutherland, J.B. Meddings, Gastroenterol **104**, 1627–1632 (1993)

H.J. Kim, D. Huh, G. Hamiltonan, D.E. Ingber, Lab Chip **12**, 2165–2174 (2012)

J. Ando, K. Yamamoto, Cardiovasc. Res. **99**, 260–268 (2013)

M. Ikenouchi, K. Furuse, H. Furuse, S. Sasaki, S. Tsukita, J. Tsukita, Cell Biol. **171**, 939–945 (2005)

J.R. Pappenheimer, Am. J. Physiol. **265**, G409–G417 (1993)

K.R. Groschwitz, S.P. Hogan, J. Allergy. Clin. Immunol. **124**, 3–20 (2009)

H. Ting, J.R. Jahn, J.I. Jung, B.R. Shuman, S. Feghhi, S.J. Han, M.L. Rodriguez, N.J. Sniadecki, Am. J Physiol. Heart. Circ. Physiol. **302**, H2220–H2229 (2012)

L.S. Gan, D.R. Thakker, Adv. Drug Del. Rev. **23**, 77–98 (1997)

M. Furuse, K. Fujita, T. Hiragi, S. Tsukita, J. Cell Biol. **141**, 1539–1550 (1998)

M.T. Furuse, M. Hirase, M. Itoh, A. Nagafuchi, S. Yonemura, S. Tsukita, S. Tsukita, J. Cell Biol. **123**, 1777–1788 (1993)

M. Yazdanian, S.L. Glynn, J.L. Wright, A. Hawi, Pharm. Res. **15**, 1490–1494 (1998)

Q. Ramadan, H. Jafarpoorchekab, P. Silacci, S. Carrara, J. Ramsden, G. Vergeres, M.A.M. Gijs, Lab Chip **13**, 196–203 (2013)

M. Brand, T.L. Hannah, C. Muller, Y. Cetin, F.G. Hamel, Ann. Biomed. Eng. **28**, 1210–1217 (2000)

C. Resta-Lenert, K.E. Barrett, Ann. N.Y. Acad. Sci. **1165**, 175–182 (2009)

S. Guo, R. Al-Sadi, H.M. Said, T.Y. Ma. Am. J. Pathol. **182**(2), 375–387 (2013)

W.V. Graham, A.M. Marchiando, L. Shen, J.R. Turner, Ann. N.Y. Acad. Sci. **1165**, 314–322 (2009)